Article

T-Cells Rich Classical Hodgkin Lymphoma, a Pathology Diagnostic Pitfall for Nodular Lymphocyte-Predominant Hodgkin Lymphoma; Case Series and Review

Haneen Al-Maghrabi *[ID], Ghadeer Mokhtar and Ahmed Noorsaeed

Department of Pathology and Laboratory Medicine, King Faisal Specialist Hospital and Research Center, P.O. Box 40047, Jeddah 21499, Saudi Arabia
* Correspondence: almaghrabi.han@gmail.com; Tel.: +966-012-667-7777

Abstract: Background: Some cases of classic Hodgkin lymphoma (CHL) display similarities to nodular lymphocyte predominant Hodgkin lymphoma (NLPHL) in terms of architecture, leading to potential challenges in diagnosis. However, these difficulties can be overcome by conducting a thorough set of immunohistochemical examinations. Objective: To examine cases of T-cell-rich CHL that closely resemble the diagnosis of NLPHL, specifically pattern D, which can pose challenges in accurately determining the diagnosis even after conducting a thorough immunophenotypic assessment. Materials and methods: Histopathology slides of three cases of T-cell-rich CHL were retrieved and thoroughly examined to assess their clinical, immunomorphologic, and molecular features. Results: We present three cases containing cells that resembled lymphocyte predominant and Hodgkin Reed–Sternberg cells, expressing some B-cell antigens and CHL markers but all were lacking Epstein–Barr virus-encoded small RNA. All three cases were found in a background rich in T-cells with focal remaining follicular dendritic cell meshwork in one case. Only one case had few eosinophils while the other two had no background of eosinophils and plasma cells. Two patients presented with stage IIA and B-symptoms presented in one of them. Two patients were treated with four and six cycles of ABVD (doxorubicin, bleomycin, vinblastine, and dacarbazine), respectively. One patient planned to be treated with four cycles of ABVD plus Rituximab therapy. Conclusions: Some cases of Reed–Sternberg cells can show expression of both B-cell and CHL markers. This overlapping characteristic, which has not been extensively discussed in the existing literature, presents a unique challenge for treatment. Further research into these neoplasms may reveal valuable diagnostic and therapeutic implications.

Keywords: classical Hodgkin lymphoma; nodular lymphocytes predominant; immunohistochemistry; lymphoma; hematopoietic

1. Introduction

According to the 5th edition of the World Health Organization (WHO) classification [1], nodular lymphocyte-predominant Hodgkin lymphoma (NLPHL) or nodular lymphocyte-predominant (LP) B-cell lymphoma, as classified by the international consensus classification (ICC) [2], can be categorized into six groups as the following: patterns A and B (the typical patterns) and other histopathologic variant patterns (C, D, E, and F). Most patients with a typical growth pattern tend to have a slow disease progression, while those with variant patterns are more likely to experience advanced-stage or higher disease relapse rates [3]. Classic Hodgkin lymphoma (CHL) comprises four distinct histopathological variants known as nodular sclerosis, mixed cellularity, lymphocyte-rich, and lymphocyte-depleted. Lymphocyte-rich CHL subtype occurs at a rate comparable to NLPHL, making up approximately 5% of all CHL incidence. The median age of patients with lymphocyte-rich CHL is comparable to that of patients with NLPHL and is notably higher than what is seen in patients with nodular sclerosis CHL [1]. The clinical characteristics of lymphocyte-rich CHL and NLPHL are comparable, as a majority of lymphocyte-rich CHL patients exhibit

stage I or II disease and seldom experience B symptoms. Additionally, individuals with lymphocyte-rich CHL experience fewer instances of relapse compared to patients with NLPHL [4]. Despite this, both entities have an exceptional overall survival rate. A subset of cases of NLPHL and CHL can appear very similar in terms of histomorphology, especially in small biopsy samples. Additionally, prior recognition of a significant similarity between instances of NLPHL and lymphocyte-rich CHL has prompted some to describe lymphocyte-rich CHL as a transitional stage between CHL and NLPHL [5,6]. Interestingly, the presence of octamer binding protein 2 (OCT2) and B-cell-specific octamer binding protein-1 (BOB1) has been observed to be more common in the Reed–Sternberg (RS) cells of lymphocyte-rich CHL compared to other types of CHL [6]. Unlike other types of CHLs, lymphocyte-rich CHL cases may have rosettes containing T-follicular helper (TFH) cells with an immunophenotype of programmed death-1 (PD-1)/CD279 and CD57 surrounding the neoplastic cells, in up to 50% of cases [6]. While some morphologic characteristics may be deceptive, distinguishing between these two entities can usually be achieved by conducting immunohistochemical studies and utilizing a range of antibody panels, including CD30, CD15, CD20, CD79a, and PAX5, along with in situ hybridization for Epstein–Barr virus (EBV)-encoded small RNA (EBER) [7]. In this study, we report three cases of CHL showing overlapping features between NLPHL and T-cell-rich CHL. Despite thorough examination of excisional biopsy specimens with extensive immunohistochemical analyses, a clear distinction between these subtypes can be challenging.

2. Results

A summary of the clinical and immunomorphologic characteristics of all three cases is provided in Table 1. Only one patient exhibited systemic B-symptoms. One patient was diagnosed with clinical stage I disease, while two others were diagnosed with stage II A disease. All three cases displayed a combination of morphologic features characteristic of both CHL and NLPHL. Flow cytometry analysis was conducted on case number three, as previously mentioned, using sufficient material. There was no indication of an abnormal T-cell population. Additionally, the proportion of double positive CD4/CD8 T-cells was below 0.50%, and the CD4:CD8 ratio was 16.70. On histopathology lymph node tissue, low-power examination of the three cases showed lymph nodes replaced by vague nodules with disrupted networks of follicular dendritic meshwork (Figures 1A and 2A). Residual lymphoid germinal centers were present in one case only, which is evident at the periphery of the nodule (Figure 2B). Dense T-cell-type lymphocyte infiltrates were seen in all three cases. All cases exhibited cytomorphology characteristics resembling LP and RS cells, with prominent T-cells rosetting the formation of small lymphocytes around the target cells (Figures 1C and 2C). Only one case had scattered eosinophils and plasma cells (Figure 3A), and the others contained dense lymphocytes (Figure 1B). Immunohistochemical studies were conducted in all three cases, which revealed positive B-cell markers in neoplastic cells, such as CD20 (in one case) (Figure 3D) and CD79a (in two cases). PAX5 showed dim positivity in two cases, while strong nuclear intensity in a subset of neoplastic cells in one case (Figures 1D and 3C). CD30 shows strong membranous and Golgi patterns of immune expression in all three cases (Figures 2D and 3B). CD15 and MUM1 show positive reactions in all three cases. However, they were all negative for OCT2, BOB1, and EBER. CD45 was negative in two cases and showed partial positivity in a subset of one case. CD3 and CD4 easily highlighted a rich T-cell background in all three cases (Figures 1C and 2C, respectively). CD23 and CD21 showed disrupted dendritic follicular meshwork in all submitted cases and focal residual germinal center in one case. The outcomes of the TRG, TRB, IGH, and gene rearrangements obtained through PCR are summarized at the bottom of Table 1. The PCR tests for TRG and TRB rearrangements were negative for T-cell clones in all three cases. However, PCR analysis for case one IGH rearrangement produced no results due to limited testing material. Upon repeating the test, the outcomes remained unchanged. In the second case, PCR results showed positive IGH rearrangement for B-cell clones. In the third case, PCR testing showed weak positivity for IGH rearrangements in B-cell clones.
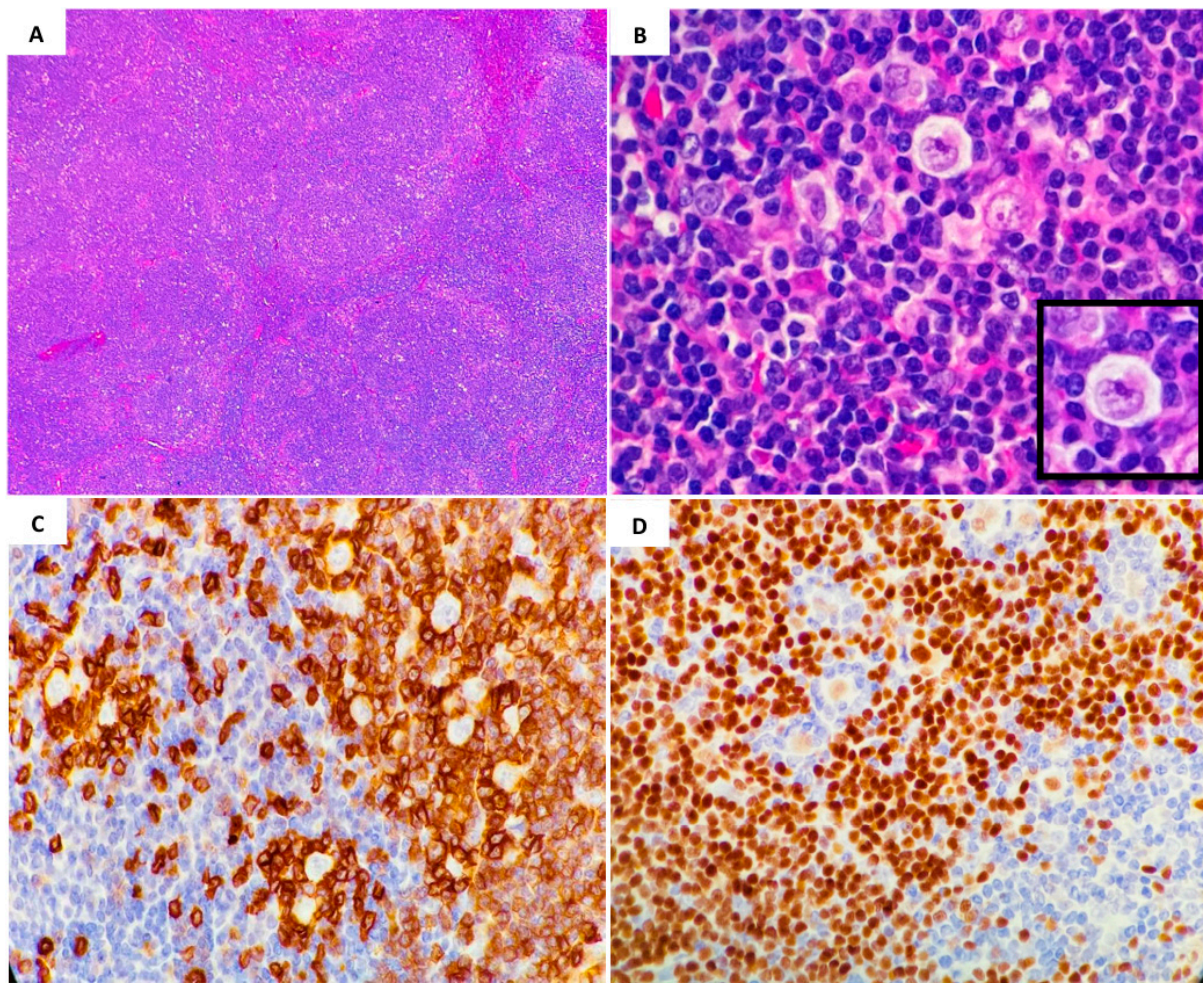
Figure 1. Histopathology examination by hematoxylin and eosin stain (H&E) and immunohistochemistry studies of case number one. (**A**): Lymph nodes show total effacement of nodal architecture by vague nodules, and no remaining reactive lymphoid follicles detected (H&E; 4×). (**B**): Reed–Sternberg (RS)-like cells present, no background of eosinophils nor plasma cells (H&E; 40×). T-cells forming a ring around the neoplastic cells are observed (inset). (**C**): CD3 immunohistochemistry stain of T-cells in the background forming a rosette around the neoplastic cells (40×). (**D**): Target cells showing weak PAX5 nuclear expression compared to the background small non-neoplastic B-cells (40×).

Table 1. Clinicopathologic features of the three cases diagnosed as classical Hodgkin lymphoma (CHL) with mixed histological features between classic Hodgkin Lymphoma and nodular lymphocyte-predominant Hodgkin lymphoma (NLPHL). EBER: Epstein–Barr virus (EBV)-encoded small RNA; ABVD: doxorubicin, bleomycin, vinblastine, and dacarbazine.

	Case 1	Case 2	Case 3
Age (year)/sex	39 y/Female	16 y/Female	34 y/Male
Stage	IIA	IIA	I
B-symptoms	No	No	Fever, loss of weight
Location	Left neck lymph node	Left supraclavicular	Right iliac lymph node
LP-like cells	Present	Present	Present
T-cell Rosette	Present	Present	Present
Residual germinal center	No	Yes	No
CD3 positive T-cell rich background	Present	Present	Present
Inflammatory cells background (Eosinophils and plasma cells)	No	No	Present
CD45	Negative	Negative	Partial positivity

Table 1. *Cont.*

|	Case 1	Case 2	Case 3
CD20	Negative	Negative	Partial positivity
CD79a	Partial positivity	Negative	Partial positivity
PAX5	Dim positive	Dim positive	Strong positive/subset
CD30	Positive	Positive	Positive/subset
CD15	Positive	Positive	Positive
CD3	Positive T-cells rich	Positive T-cells rich	Positive T-cells rich
BOB1	Negative	Negative	Negative
OCT2	Negative	Negative	Negative
EBER	Negative	Negative	Negative
IGH rearrangement by PCR testing	Scant material, no result (repeated twice)	Positive	Weak positive
TRG rearrangement by PCR testing	Negative	Negative	Negative
TRB rearrangement by PCR testing	Negative	Negative	Negative
Treatment	Surgical excision followed by 4 cycles ABVD	Surgical excision followed by 6 cycles ABVD	Surgical excision followed by 4 cycles ABVD + Rituximab
Radiation therapy	No	No	No
Clinical outcome and latest follow up	Complete remission after 1 year	Complete remission after 9 months	Complete remission after 11 months
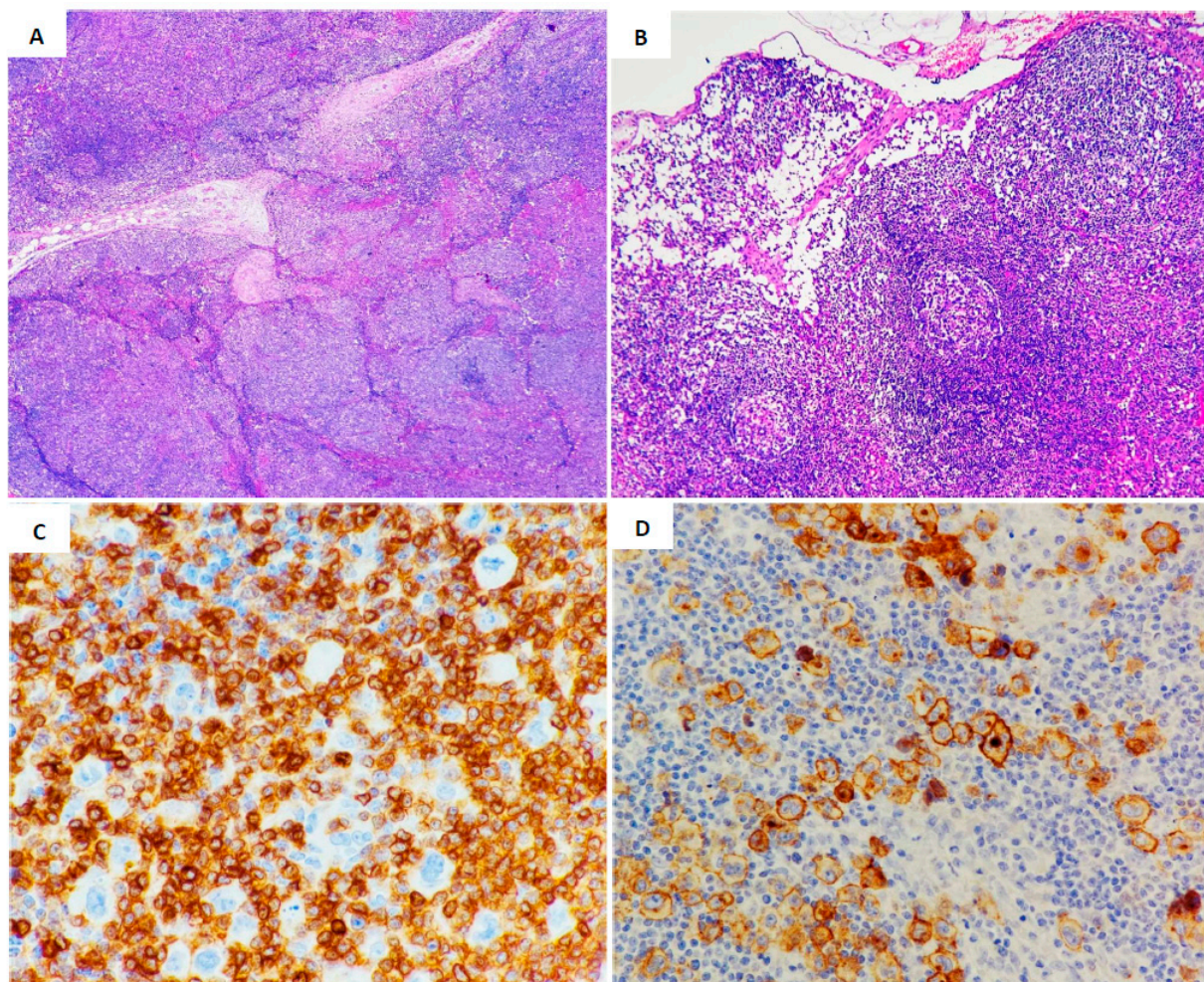
Figure 2. Histopathology examination by hematoxylin and eosin stain (H&E) and immunohistochemistry studies of case number two. (**A**): Lymph nodes show partial nodal effacement of architecture by large vague nodules (H&E; 4×). (**B**): Focal remaining reactive lymphoid follicles are detected at the

periphery of the lymph node (H&E; 40×). (**C**): CD4 immunohistochemistry stain of T-cells in the background forming a rosette around the target cells (40×). (**D**): Target cells showing CD30 membranous and Golgi positive expression (40×).
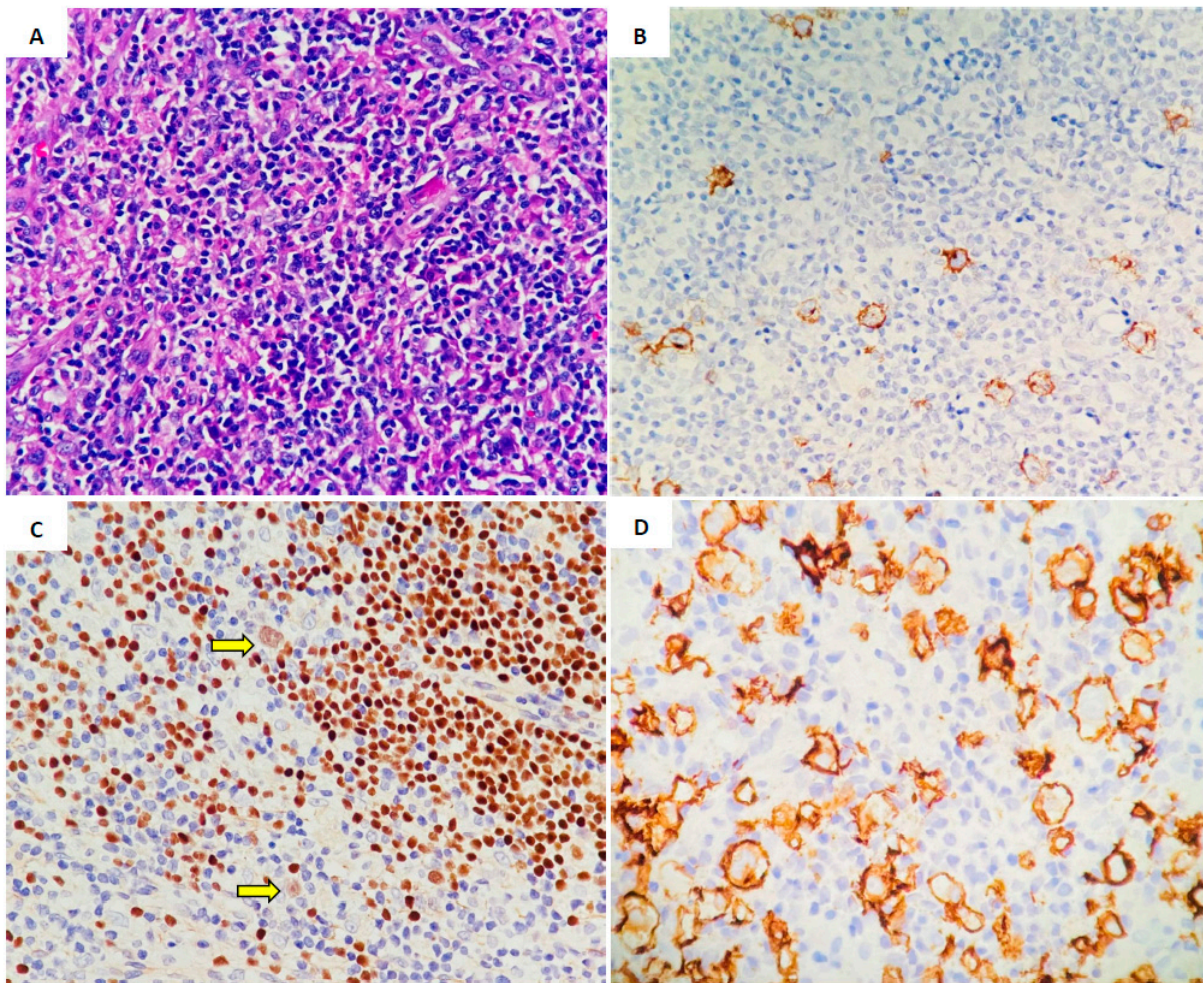

Figure 3. Histopathology examination by hematoxylin and eosin stain (H&E) and immunohistochemistry studies of case number three. (**A**): Disturbed normal lymphoid tissue by neoplastic Reed–Sternberg (RS)-like cells (very scattered), the background of eosinophils and rare plasma cells are seen (H&E; 40×). (**B**): Target cells showing CD30 membranous and Golgi positive expression (10×). (**C**): Some of the target cells show dim PAX5 nuclear expression compared to the background small non-neoplastic B-cells (arrow) (40×). (**D**): Target cells showing strong CD20 membranous positive expression in a background rich in T-cells (40×).

3. Materials and Methods

We reviewed excisional lymph node biopsies from three patients diagnosed as T-cell-rich CHL with features mimicking NLPHL. All three patients were diagnosed and managed at our institution. Flow cytometry immunophenotyping assays were carried out on the third case only using BD FACS Canto II cytometers from BD Biosciences, and the data were analyzed with FCS Express 6 software (De Novo Software). Unfortunately, cases one and two did not include flow cytometry results as they were referred from an external facility and had not submitted them for testing. The case tested for surface antigens including CD2, CD3, CD4, CD5, CD7, CD8, CD10, CD219, CD20, CD34, CD38, CD45, CD56, CD200, and T-cell receptor (TCR) gamma delta (γδ) and alpha (α) and beta (β). Histological preparations of high quality were conducted to examine tissue sections on pathology slides. These slides were stained with hematoxylin and eosin (H&E) and were prepared from tissue samples fixed and embedded in paraffin blocks. Immunohistochemical studies using

paraffin-embedded tissue sections were performed on all cases using automated antibodies (Leica Biosystems). The following immunes and probes were completed on case number one: CD45 (LCA), CD20, PAX5, CD79a, BOB1, CD15, CD30, CD3, CD4, CD23, MUM1, and EBER. The remaining two cases tested for antibodies including CD45, CD20, PAX5, BOB1, OCT2, CD30, CD15, and EBER. Moreover, polymerase chain reaction (PCR) was conducted on all three cases to amplify the immunoglobulin heavy chain (IGH) as well as the T-cell receptors gamma (TRG) and beta (TRB). The resulting PCR products were analyzed using capillary electrophoresis on an ABI PRISM® 3500 Genetic Analyzer (Foster City, CA, USA).

4. Discussion

CHL and NLPHL originate from germinal center B-cells, but they exhibit unique pathogenesis and biological characteristics that result in distinct immunophenotypes. In NLPHL, LP cells display a persistent B-cell phenotype characterized by the expression of strong PAX5, CD20, OCT2, and BOB1. On the other hand, Reed–Sternberg (RS) cells in CHL typically exhibit a lack of CD20, OCT2, and/or BOB1, with dim expression of PAX5 [8]. Presumably, LP cells in NLPHL originate from specific germinal that have undergone somatic hypermutation and intraclonal diversity in their clonal immunoglobulin (Ig) at a molecular level. This process is likely influenced by germinal center reactions that ultimately result in the maintained expression of a B-cell program receptor [9]. Additionally, LP cells engage with PD1-immune reactive T-cells to create surrounding rosettes, suggesting that this interaction could be a factor in the development of pathogenesis within the NLPHL microenvironment [10]. In contrast, RS cells in CHL originate from specific B-cell germinal centers containing clonal Ig rearrangement marked by a high somatic mutation burden in their gene. The presence of these harmful mutations typically leads to programmed cell death through cellular apoptosis. However, RS cells can survive by altering their signaling pathways to promote survival and evade immune responses, including signals from NF-kB and JAK/STAT pathways, as well as signals from EBV infection [9,10]. On a molecular level, gene expression profiling has revealed a strong correlation between target cells of CHL and NLPHL, indicating a decrease in B-cell gene activity and lower expression of B-cell-specific transcription expression. Furthermore, both LP cells and RS cells have demonstrated nuclear factor kB (NF-kB) activity and activation of the extracellular regulated kinase (ERK) signaling pathway [11].

The similarity in cytomorphology between cases of NLPHL (patterns A, B, and C) and lymphocyte-rich CHL is well-documented. Both conditions exhibit nodules of B-cells that are believed to originate from the mantle zone of lymphoid follicles, with TFH-cells forming a rosette around neoplastic RS or LP cells. Additionally, both conditions typically lack eosinophils or neutrophils [7,8]. The cases examined in this study stood out due to their T-cell-rich nodules, which closely resembled pattern D of NLPHL. TFH-cell rosettes were evident in two cases but were only observed in a limited area in the remaining case based on immunohistochemistry staining. In one case, the focal background of eosinophils and neutrophils was present, while they were not observed in the other two cases. A recently confirmed finding is that LP cells in NLPHL may exhibit a diminished B-cell program, resembling the RS cells in CHL, with certain characteristics such as lacking CD20 and potentially expressing CD30 and CD15 [12–14]. Subset of NLPHL (patterns A, B, and C) and B-cell-rich CHL can exhibit similar cytomorphological features, which may also display partially overlapping immunophenotypic results [7]. However, using a comprehensive set of immunohistochemical markers and in situ hybridization study for EBV can often be beneficial in differentiating between these two pathologic diagnoses. On the other hand, in the T-cell predominant CHL cases we describe, the target neoplastic cells show a mixed feature of incomplete to lack of expression of several B-cell markers typically found in NLPHL (CD20, CD79a) as well as CHL expression as (CD30, CD15, and dim nuclear PAX5). The contribution of EBV to the development of NLPHL is not as well understood as in CHL, where EBV-positive cases have been found to have a higher mutational burden than EBV-negative cases [15]. Despite this, EBV may still be present in approximately 5% of

NLPHL cases [16]. The presence of EBV in NLPHL adds to the challenge of distinguishing it from EBV-positive CHL cases, especially since EBV pathogenesis usually increases the expression of CD30 [17]. None of the cases we presented displayed any evidence of EBER. In the three cases examined, there was a decrease or loss of expression of B-cell markers including CD20, CD79a, and BOB1. Only one case revealed CD20 expression along with a lack of a significant CD4/CD8 double-positive T-cell population as determined by flow cytometry analysis suggests that the diagnosis of NLPHL with a T-cell-rich background is unlikely.

The variable nuclear expression of PAX5 staining could influence the overall clinical survival of the disease. While the reason for the absence of PAX5 staining in rare cases of CHL remains unclear, a limited study involving PAX5-negative CHL cases indicated that these patients might experience poorer clinical outcomes compared to those with typical PAX5-positive CHL. Specifically, they seem to have a higher likelihood of relapse or a shorter duration of progression-free survival [18]. The clinical efficacy of anti-CD30 antibodies has been somewhat limited. Moreover, their combinations with bacterial toxins and radioimmunoconjugates have yielded only modest outcomes. Nevertheless, the emergence of the antibody–drug conjugate brentuximab vedotin (BV) has rekindled interest in targeting CD30 as a tumor marker. It has also been proposed that the varying response to anti-CD30 antibodies in CHL could indicate a prosurvival advantage that is influenced by the unique microenvironment of CHL. This hypothesis is supported by the observation of a "bystander" effect on adjacent non-CD30-positive cells, which might modify the immune signaling within the CHL microenvironment [19]. Moreover, a viral infection can trigger the activation of CD30 in both B and T-cells. Cells infected with the EBV may also exhibit this activation [18,19].

Beyond the scope of CHL, differential diagnoses could be T-cell histiocyte-rich large B-cell lymphoma (THRBCL), gray-zone lymphoma (GZL), and nodal TFH cell lymphoma, follicular type [19]. The lack of histiocytic background and the presence of follicular dendritic cell meshwork suggest that the diagnosis of THRBCL is less likely. In contrast to the cases we presented, GZL that resembles primary mediastinal B-cell lymphoma typically presents as a uniform large, atypical cell, with medium to large size target cells in a dense fibrotic stroma that may have scant to rare inflammatory cells. Nodal TFH cell lymphoma was ruled out in all three cases due to the lack of the following: atypical T-cells that typically contain pale to clear cytoplasm, high endothelial venules proliferation, and vascular wall hyalinized basement membranes, along with the absence of aberrant T-cell marker expression by flow cytometry analysis completed on available material. Therefore, considering all these factors, we believe that our represented cases are of CHL that share some characteristic features of NLPHL- T-cell rich nodular (pattern D) [16,17,19].

Ultimately, CHL is characterized by a significant immune infiltrate, which plays a fundamental role in the neoplastic process. The HRS cells foster an immunosuppressive microenvironment through the expression of regulatory molecules, inhibiting T-cell activation. In a study utilizing tissue samples for single-cell RNA sequencing (scRNA-seq) analysis, the classical monocytes function as crucial signaling hubs. They may regulate the retention of cDC2 and ThExh through CCR1-, CCR4-, CCR5-, and CXCR3-dependent signaling pathways. The enrichment of the cDC2–monocyte–macrophage network in diagnostic biopsies correlates with early treatment failure. These findings highlight unexpected complexity and spatial polarization within the mononuclear phagocyte (MNP) compartment, further underscoring their potential roles in immune evasion by CHL [20].

5. Conclusions

We present three cases of CHL, T-cell rich background demonstrating characteristics shared by NLPHL and lymphocyte-rich CHL. In contrast with the similarity observed in B-cell-rich CHL and NLPHL, particularly in patterns A, B, and C which share the feature of B-cell-rich nodules, the three cases we are presenting had a predominance of T-cells, like NLPHL pattern D. These cases contained LP-like cells resembling those

found in NLPHL, along with partial expression of B-cell surface antigen and CHL markers. T-cell rosettes were observed around the target cells in all three cases, resembling NLPHL. One case showed a focal background of eosinophils and plasma cells, while another case exhibited residual germinal centers as seen in CHL. These instances further highlight the role of related pathogenesis between LP and HRS cells. This highlights the importance of further examining similar cases of T-lymphocyte-rich CHL with overlapping immunophenotypes to identify unique characteristics that could have diagnostic or therapeutic clinical implications.

References

1. Alaggio, R.; Amador, C.; Anagnostopoulos, I.; Attygalle, A.D.; Araujo, I.B.; Berti, E.; Bhagat, G.; Borges, A.M.; Boyer, D.; Calaminici, M.; et al. The 5th edition of the World Health Organization Classification of Haematolymphoid Tumours: Lymphoid neoplasms. *Leukemia* **2022**, *36*, 1720–1748. [CrossRef] [PubMed]
2. Campo, E.; Jaffe, E.S.; Cook, J.R.; Quintanilla-Martinez, L.; Swerdlow, S.H.; Anderson, K.C.; Brousset, P.; Cerroni, L.; de Leval, L.; Dirnhofer, S.; et al. The international consensus classification of mature lymphoid neoplasms: A report from the clinical advisory committee. *Blood* **2022**, *140*, 1229–1253. [CrossRef]
3. Shankar, A.G.; Kirkwood, A.A.; Hall, G.W.; Hayward, J.; O'Hare, P.; Ramsay, A.D. Childhood and adolescent nodular lymphocyte predominant Hodgkin lymphoma—A review of clinical outcome based on the histological variants. *Br. J. Haematol.* **2015**, *171*, 254–262. [CrossRef] [PubMed]
4. Diehl, V.; Sextro, M.; Franklin, J.; Hansmann, M.L.; Harris, N.; Jaffe, E.; Poppema, S.; Harris, M.; Franssila, K.; Van Krieken, J.; et al. Clinical presentation, course, and prognostic factors in lymphocyte-predominant Hodgkin's disease and lymphocyterich classical Hodgkin's disease: Report from the European Task Force on Lymphoma Project on Lymphocyte-Predominant Hodgkin's Disease. *J. Clin. Oncol.* **1999**, *17*, 776–783. [CrossRef]
5. El Hussein, S.; Wang, X.; Fang, H.; Jelloul, F.Z.; Wang, W.; Loghavi, S.; Medeiros, L.J. Nodular lymphocyte-predominant Hodgkin lymphoma with nodular sclerosis: An underrecognized feature associated with pattern D. *Am. J. Surg. Pathol.* **2022**, *46*, 1291–1297. [CrossRef]
6. Nam-Cha, S.H.; Montes-Moreno, S.; Salcedo, M.T.; Sanjuan, J.; Garcia, J.F.; Piris, M.A. Lymphocyte-rich classical Hodgkin's lymphoma: Distinctive tumor and microenvironment markers. *Mod. Pathol.* **2009**, *22*, 1006–1015. [CrossRef]
7. O'Malley, D.P.; Dogan, A.; Fedoriw, Y.; Medeiros, L.J.; Ok, C.Y.; Salama, M.E. American Registry of Pathology expert opinions: Immunohistochemical evaluation of classic Hodgkin lymphoma. *Ann. Diagn. Pathol.* **2019**, *39*, 105–110. [CrossRef] [PubMed]
8. Anagnostopoulos, I.; Hansmann, M.L.; Franssila, K.; Harris, M.; Harris, N.L.; Jaffe, E.S.; Stein, H. European Task Force on Lymphoma project on lymphocyte predominance Hodgkin disease: Histologic and immunohistologic analysis of submitted cases reveals 2 types of Hodgkin disease with a nodular growth pattern and abundant lymphocytes. *Blood* **2000**, *96*, 1889–1899. [PubMed]
9. Cirillo, M.; Reinke, S.; Klapper, W.; Borchmann, S. The translational science of Hodgkin lymphoma. *Br. J. Haematol.* **2019**, *184*, 30–44. [CrossRef] [PubMed]
10. Hartmann, S.; Scharf, S.; Steiner, Y.; Loth, A.G.; Donnadieu, E.; Flinner, N.; Hansmann, M.L. Landscape of 4D cell interaction in Hodgkin and non-Hodgkin lymphomas. *Cancers* **2021**, *13*, 5208. [CrossRef] [PubMed]
11. Brune, V.; Tiacci, E.; Pfeil, I.; Döring, C.; Eckerle, S.; Van Noesel, C.J.; Küppers, R. Origin and pathogenesis of nodular lymphocyte-predominant Hodgkin lymphoma as revealed by global gene expression analysis. *J. Exp. Med.* **2008**, *205*, 2251–2268. [CrossRef]

12. Menke, J.R.; Spinner, M.A.; Natkunam, Y.; Warnke, R.A.; Advani, R.H.; Gratzinger, D.A. CD20-negative nodular lymphocyte-predominant Hodgkin lymphoma: A 20-year consecutive case series from a tertiary cancer center. *Arch. Pathol. Lab. Med.* **2021**, *145*, 753–758. [CrossRef] [PubMed]

13. Seliem, R.M.; Ferry, J.A.; Hasserjian, R.P.; Harris, N.L.; Zukerberg, L.R. Nodular lymphocyte-predominant Hodgkin lymphoma (NLPHL) with CD30-positive lymphocyte- predominant (LP) cells. *J. Hematop.* **2011**, *4*, 175. [CrossRef] [PubMed]

14. Venkataraman, G.; Raffeld, M.; Pittaluga, S.; Jaffe, E.S. CD15-expressing nodular lymphocyte-predominant Hodgkin lymphoma. *Histopathology* **2011**, *58*, 803–805. [CrossRef] [PubMed]

15. Wienand, K.; Chapuy, B.; Stewart, C.; Dunford, A.J.; Wu, D.; Kim, J.; Shipp, M.A. Genomic analyses of flow-sorted Hodgkin Reed-Sternberg cells reveal complementary mechanisms of immune evasion. *Blood Adv.* **2019**, *3*, 4065–4080. [CrossRef] [PubMed]

16. Huppmann, A.R.; Nicolae, A.; Slack, G.W.; Pittaluga, S.; Davies-Hill, T.; Ferry, J.A.; Hasserjian, R.P. EBV may be expressed in the LP cells of nodular lymphocyte-predominant Hodgkin lymphoma (NLPHL) in both children and adults. *Am. J. Surg. Pathol.* **2014**, *38*, 316–324. [CrossRef] [PubMed]

17. El Hussein, S.; Shaw, K.R.M.; Vega, F. Evolving insights into the genomic complexity and immune landscape of diffuse large B-cell lymphoma: Opportunities for novel biomarkers. *Mod. Pathol.* **2020**, *33*, 2422–2436. [CrossRef] [PubMed]

18. Jaffe, E.S. Anaplastic large cell lymphoma: The shifting sands of diagnostic hematopathology. *Mod. Pathol.* **2001**, *14*, 219–228. [CrossRef] [PubMed]

19. Younes, S.; Rojansky, R.B.; Menke, J.R.; Gratzinger, D.; Natkunam, Y. Pitfalls in the diagnosis of nodular lymphocyte predominant Hodgkin lymphoma: Variant patterns, borderlines and mimics. *Cancers* **2021**, *13*, 3021. [CrossRef] [PubMed]

20. Stewart, B.J.; Fergie, M.; Young, M.D.; Jones, C.; Sachdeva, A.; Blain, A.; Carey, C.D. Spatial and molecular profiling of the mononuclear phagocyte network in classic Hodgkin lymphoma. *Blood J. Am. Soc. Hematol.* **2023**, *141*, 2343–2358. [CrossRef] [PubMed]